

Curvature of Quantum Evolutions for Qubits in Time-Dependent Magnetic Fields

Carlo Cafaro^{1,2}, Leonardo Rossetti^{3,1}, Paul M. Alsing¹

¹*University at Albany-SUNY, Albany, NY 12222, USA*

²*SUNY Polytechnic Institute, Utica, NY 13502, USA and*

³*University of Camerino, I-62032 Camerino, Italy*

In the geometry of quantum-mechanical processes, the time-varying curvature coefficient of a quantum evolution is specified by the magnitude squared of the covariant derivative of the tangent vector to the state vector. In particular, the curvature coefficient measures the bending of the quantum curve traced out by a parallel-transported pure quantum state that evolves in a unitary fashion under a nonstationary Hamiltonian that specifies the Schrödinger evolution equation. In this paper, we present an exact analytical expression of the curvature of a quantum evolution for a two-level quantum system immersed in a time-dependent magnetic field. Specifically, we study the dynamics generated by a two-parameter nonstationary Hermitian Hamiltonian with unit speed efficiency. The two parameters specify the constant temporal rates of change of the polar and azimuthal angles used in the Bloch sphere representation of the evolving pure state. To better grasp the physical significance of the curvature coefficient, showing that the quantum curve is nongeodesic since the geodesic efficiency of the quantum evolution is strictly less than one and tuning the two Hamiltonian parameters, we compare the temporal behavior of the curvature coefficient with that of the speed and the acceleration of the evolution of the system in projective Hilbert space. Furthermore, we compare the temporal profile of the curvature coefficient with that of the square of the ratio between the parallel and transverse magnetic field intensities. Finally, we discuss the challenges in finding exact analytical solutions when extending our geometric approach to higher-dimensional quantum systems that evolve unitarily under an arbitrary time-dependent Hermitian Hamiltonian.

PACS numbers: Quantum Computation (03.67.Lx), Quantum Information (03.67.Ac), Quantum Mechanics (03.65.-w), Riemannian Geometry (02.40.Ky).

I. INTRODUCTION

The dynamical evolution of quantum systems entails two main challenges [1]. First, focusing on the Schrödinger evolution equation for two-level systems, the mathematics is not always transparent and the complex coefficients that appear in the wave function do not give directly the values of real physical observables. Second, even for two-level systems, there is a limited applicability of analytical techniques for exactly solving the Schrödinger evolution equation. Therefore, numerical estimations are necessary in many realistic cases. However, it is generally difficult to gain general insights about the dependence of the system on its tunable parameters while performing exclusively numerical investigations. In this respect, geometrical methods can offer useful tools, since they can help with pictorial visualizations of quantum interactions. These visualizations, in turn, can lead to the possibility of gaining deeper insights into the physics of the problem at hand. Furthermore, geometry offers the chance of handling relatively simple concepts formulated in terms of ordinary real scalar and vectorial quantities with a transparent interpretation. Therefore, in principle, the possibility of exploiting the power of simple geometrical quantities to characterize aspects of complicated quantum-mechanical phenomena can be of great theoretical and practical relevance.

Relying on the very clever conversion of the (complex) two-level Schrödinger equation to (real) vectorial three-dimensional spin precession equation by Feynman and collaborators in Ref. [1], there have been fascinating studies on the consequences of mapping quantum-mechanical two-level systems to a space curve [2–4]. In this context, making use of suitable methods of differential geometry such as the Frenet-Serret equations, scientists have provided interesting geometric descriptions of certain aspects of quantum evolutions by means of the concepts of curvature and torsion of a space curve. In Ref. [2], for instance, the curvature of the space curve is related to the variance of the Hamiltonian. Furthermore, a measure of the deviation of the torsion of the curve from an instantaneous osculating plane is related to the geometric phase of the quantum evolution corresponding to the two-level system. In Ref. [3], the authors express the curvature and the torsion of the space curve in terms of the Hamiltonian of the quantum system. Then, from the study of the behavior of these two geometric quantities, an efficient way of classifying different families of quantum systems and processes (including, for instance, two-level atoms, spin-1/2 particles, Rosen-Zener systems, and electronic transitions) was suggested. Finally, using the above-mentioned Frenet-Serret frame of a space curve, the authors provide in Ref. [4] classical analogues of the Schrödinger and Heisenberg pictures in quantum mechanics. In addition to its clear foundational relevance, this line of investigation has recently found space for practical importance in the context of optimal driving of quantum systems with minimal energy consumption [5]. Currently, the impact that the concepts of geometric curvature and torsion can have on the future of quantum technology for superconducting

spintronics devices is being seriously investigated [6].

In differential geometry, it is established that the classical Frenet-Serret apparatus of a space curve in three-dimensional Euclidean space specifies the local geometry of curves [7]. In particular, it characterizes relevant geometric invariants, including the curvature and the torsion of a curve. Observe that the notion of curvature of a space curve in three-dimensional Euclidean space as introduced in classical differential geometry (by the Frenet-Serret curvature coefficient κ_{FS}) is well-defined in a flat space where no gravity is present. In classical Newtonian mechanics, physicists can describe geometric aspects of classical trajectories of a particle by means of curvature and torsion coefficients presented within the Frenet-Serret apparatus. As a side remark, we stress that the first scientist to consider the geometrization of Newtonian gravity was Cartan [8]. In Ref. [9], for instance, curvature and torsion coefficients of a space curve were employed to study the geometry of the cylindrical helix motion of a spin-1/2 charged particle in a homogeneous external magnetic field. Since the curvature of a space curve can be expressed in terms of velocity and acceleration [7], it is reasonable to expect that the temporal rate of change of the curvature is somewhat related to the time-derivative of the acceleration, also known as the jerk. For an interesting discussion on the jerk of space curves corresponding to electrons moving in a constant magnetic field in three-dimensional Euclidean space equipped with moving Frenet-Serret frames, we refer to Refs. [10, 11].

In geometric quantum mechanics, while analyzing the problem of parameter estimation, the concept of curvature of a quantum Schrödinger trajectory was introduced in Ref. [12] as a generalization of the notion of curvature of a classical exponential family of distributions of use in statistical mechanics. In Ref. [12], the curvature of a curve can be characterized in terms of a suitably introduced squared acceleration vector of the curve. Furthermore, the curvature measures the parametric sensitivity that specifies the parametric estimation problem being studied [13]. In Ref. [14], Laba and Tkachuk defined curvature and torsion coefficients of quantum evolutions for pure states that evolved subject to a time-independent Hamiltonian evolution. Focusing on single-qubit quantum states, they showed that the curvature is a measure of the deviation of the dynamically evolving state vector from the geodesic line on the Bloch sphere in Ref. [14]. In addition, they concluded that the torsion coefficient is a measure of the deviation of the dynamically evolving state vector from a two-dimensional subspace characterized by the instantaneous plane of evolution. It is important pointing out that the concepts of Frenet-Serret curvature, geodesic curvature, and curvature coefficient of a quantum evolution encode different information about a curve. For instance, while the curvature of a circle on a plane is an intrinsic property of the circle, the curvature of a circle on a spherical surface is an extrinsic property of the circle. For simplicity, take a circle of radius R . When this circle is regarded as a great circle on a sphere, it has geodesic curvature equal to zero. Clearly, if the circle lies on the sphere but is not a great sphere, its geodesic curvature differs from zero. Moreover, the Frenet-Serret curvature of a circle at the equatorial plane of a sphere in \mathbb{R}^3 is clearly nonzero (unlike what happens when you view the circle as the equatorial trajectory on a Bloch sphere with the curvature of the quantum evolution equal to zero). For a discussion on the link among Frenet-Serret curvature, geodesic curvature, and curvature coefficient of a quantum evolution, we refer to Ref. [15].

Using the concept of Frenet-Serret apparatus and, in part, influenced by the investigation by Laba and Tkachuk in Ref. [14], we brought forward in Refs. [15–17] an alternative geometric approach to specify the bending and the twisting of quantum curves traced out by dynamically evolving state vectors in a quantum setting. Specifically, we proposed a quantum version of the Frenet-Serret apparatus for a quantum trajectory in projective Hilbert space traced out by a parallel-transported pure quantum state that evolves unitarily under a stationary (or, alternatively, nonstationary) Hamiltonian specifying the Schrödinger equation. For nonstationary Hamiltonian evolutions [16], we found that the time-varying setting exhibited a richer structure from a statistical standpoint compared to the stationary setting [15]. For instance, unlike the time-independent configuration, we found that the notion of generalized variance enters nontrivially in the definition of the torsion of a curve traced out by a quantum state evolving under a nonstationary Hamiltonian. To physically illustrate the significance of our construct, we applied it to an exactly soluble time-dependent two-state Rabi problem specified by a sinusoidal oscillating time-dependent potential. In this context, we showed that the analytical expressions for the curvature and torsion coefficients can be (in principle) completely described by only two real three-dimensional vectors, the Bloch vector that specifies the quantum system and the externally applied time-varying magnetic field. Although we demonstrated that the torsion is identically zero for an arbitrary time-dependent single-qubit Hamiltonian evolution, we only studied in a numerical fashion the temporal behavior of the curvature coefficient in different dynamical scenarios, including off-resonance and on-resonance regimes and, in addition, strong and weak driving configurations.

In this paper, the main goal is that of achieving a deeper understanding of the physical significance of the curvature coefficient of a quantum evolution for a two-level quantum system immersed in a time-dependent magnetic field by providing (for the first time in the literature, to our knowledge) an exact analytical analysis. Our objective is to handle a spectrum of inquiries, including but not limited to:

- [i] When transitioning from stationary to nonstationary Hamiltonian settings, which type of magnetic field configurations yield a vanishing curvature coefficient?

- [ii] Are energy resources necessarily wasted while bending quantum evolutions?
- [iii] How is the temporal behavior of the curvature coefficient of a quantum path related to the temporal profile of its speed and its acceleration in projective Hilbert space?

Addressing points [i], [ii], and [iii] is relevant for several reasons in the field of quantum information and computation. For instance, the proper quantitative understanding of these points can help developing suitable quantum driving schemes capable of transferring a source state to a target state in minimal time, optimal speed, and with minimal waste of energy resources.

Before presenting the layout of this paper, we stress that the notions of “time-dependent, time-varying, and non-stationary” magnetic field configurations (or, alternatively, Hamiltonian evolutions) are used as synonyms in this work.

The rest of the paper is organized as follows. In Section II, we present the essential formal elements yielding the concept of curvature of a quantum evolution. In Section III, we characterize the dynamics generated by a two-parameter time-dependent Hamiltonian with unit speed efficiency. The two parameters determine the constant temporal rates of change of the polar and azimuthal angles employed in the Bloch sphere description of the quantum-mechanical evolving pure state. In Section IV, to deepen our understanding of the concept of curvature, we study several aspects of the quantum evolution. Specifically, we show that while the nonstationary Hamiltonian corresponds to a 100% evolution speed efficiency [18], it generates nongeodesic paths on the Bloch sphere since the geodesic efficiency of the quantum evolution is strictly less than one [19, 20]. Furthermore, while tuning the two Hamiltonian parameters, we study and compare the temporal behavior of the speed and the acceleration of the evolution in projective Hilbert space with that of the curvature coefficient. Lastly, we provide a comparison between the temporal profile of the curvature coefficient with that of the square of the ratio between the parallel (i.e., along the z -axis) and transverse (i.e., in the xy -plane) magnetic field intensities. Our summary of findings along with concluding remarks appear in Section V. Finally, technical details are placed in Appendix A.

II. CURVATURE OF A QUANTUM EVOLUTION

In this section, we follow our works in Refs. [15–17] to introduce the basic elements leading to the concept of the curvature of a quantum evolution.

Consider a nonstationary Hamiltonian evolution described by the Schrödinger’s equation $i\hbar\partial_t |\psi(t)\rangle = \mathbf{H}(t) |\psi(t)\rangle$, with $|\psi(t)\rangle$ belonging to an arbitrary N -dimensional complex Hilbert space \mathcal{H}_N . Although this introductory presentation assumes that the reduced Planck constant \hbar is not one, we shall set $\hbar = 1$ throughout our paper in most of our explicit calculations. Whenever felt necessary, the choice of setting $\hbar = 1$ will be explicitly reminded to the reader. In general, the normalized state vector $|\psi(t)\rangle$ is such that $\langle \dot{\psi}(t) | \dot{\psi}(t) \rangle = (-i/\hbar) \langle \psi(t) | \mathbf{H}(t) | \psi(t) \rangle \neq 0$. Given the state $|\psi(t)\rangle$, we introduce the parallel transported unit state vector $|\Psi(t)\rangle \stackrel{\text{def}}{=} e^{i\beta(t)} |\psi(t)\rangle$ where the phase $\beta(t)$ is such that $\langle \Psi(t) | \dot{\Psi}(t) \rangle = 0$. Observe that $i\hbar |\dot{\Psi}(t)\rangle = [\mathbf{H}(t) - \hbar\dot{\beta}(t)] |\Psi(t)\rangle$. Then, the relation $\langle \Psi(t) | \dot{\Psi}(t) \rangle = 0$ is equivalent to putting $\beta(t)$ equal to

$$\beta(t) \stackrel{\text{def}}{=} \frac{1}{\hbar} \int_0^t \langle \psi(t') | \mathbf{H}(t') | \psi(t') \rangle dt'. \quad (1)$$

For this reason, $|\Psi(t)\rangle$ reduces to

$$|\Psi(t)\rangle = e^{(i/\hbar) \int_0^t \langle \psi(t') | \mathbf{H}(t') | \psi(t') \rangle dt'} |\psi(t)\rangle, \quad (2)$$

and satisfies the evolution equation $i\hbar |\dot{\Psi}(t)\rangle = \Delta\mathbf{H}(t) |\Psi(t)\rangle$ where $\Delta\mathbf{H}(t) \stackrel{\text{def}}{=} \mathbf{H}(t) - \langle \mathbf{H}(t) \rangle$. As pointed out in Ref. [16], the speed $v(t)$ of quantum evolution is not constant when the Hamiltonian is nonstationary. In particular, $v(t)$ is such that $v^2(t) = \langle \dot{\Psi}(t) | \dot{\Psi}(t) \rangle = \langle (\Delta\mathbf{H}(t))^2 \rangle / \hbar^2$. We introduce for convenience the arc length $s = s(t)$ specified by means of $v(t)$ as

$$s(t) \stackrel{\text{def}}{=} \int_0^t v(t') dt', \quad (3)$$

with $ds = v(t)dt$, that is, $\partial_t = v(t)\partial_s$. Clearly, $\partial_t \stackrel{\text{def}}{=} \partial/\partial t$ and $\partial_s \stackrel{\text{def}}{=} \partial/\partial s$. Finally, presenting the adimensional operator

$$\Delta h(t) \stackrel{\text{def}}{=} \frac{\Delta H(t)}{\hbar v(t)} = \frac{\Delta H(t)}{\sqrt{\langle (\Delta H(t))^2 \rangle}}, \quad (4)$$

the normalized tangent vector $|T(s)\rangle \stackrel{\text{def}}{=} \partial_s |\Psi(s)\rangle = |\Psi'(s)\rangle$ becomes $|T(s)\rangle = -i\Delta h(s)|\Psi(s)\rangle$. We remark that $\langle T(s)|T(s)\rangle = 1$ by construction and, in addition, $\partial_s \langle \Delta h(s) \rangle = \langle \Delta h'(s) \rangle$. Indeed, this latter relation can be extended to an arbitrary power of differentiation. To the second power, for example, we have $\partial_s^2 \langle \Delta h(s) \rangle = \langle \Delta h''(s) \rangle$. We can construct $|T'(s)\rangle \stackrel{\text{def}}{=} \partial_s |T(s)\rangle$ from the tangent vector $|T(s)\rangle = -i\Delta h(s)|\Psi(s)\rangle$. As a matter of fact, after some algebra, we obtain $|T'(s)\rangle = -i\Delta h(s)|\Psi'(s)\rangle - i\Delta h'(s)|\Psi(s)\rangle$ where

$$\langle T'(s)|T'(s)\rangle = \langle (\Delta h'(s))^2 \rangle + \langle (\Delta h(s))^4 \rangle - 2i \text{Re} \left[\langle \Delta h'(s) (\Delta h(s))^2 \rangle \right] \neq 1, \quad (5)$$

in general. We are now prepared to present the curvature coefficient for quantum evolutions generated by nonstationary Hamiltonians. Indeed, having introduced the vectors $|\Psi(s)\rangle$, $|T(s)\rangle$, and $|T'(s)\rangle$, we can finally establish the curvature coefficient $\kappa_{\text{AC}}^2(s) \stackrel{\text{def}}{=} \langle \tilde{N}_*(s) | \tilde{N}_*(s) \rangle$ with $|\tilde{N}_*(s)\rangle \stackrel{\text{def}}{=} P^{(\Psi)} |T'(s)\rangle$, where the projection operator $P^{(\Psi)}$ onto states orthogonal to $|\Psi(s)\rangle$ is given by $P^{(\Psi)} \stackrel{\text{def}}{=} I - |\Psi(s)\rangle \langle \Psi(s)|$, and “I” denotes the identity operator in \mathcal{H}_N . As mentioned in Refs. [15, 16], the subscript “AC” means Alsing and Cafaro. Observe that the curvature coefficient $\kappa_{\text{AC}}^2(s)$ can be recast as

$$\kappa_{\text{AC}}^2(s) \stackrel{\text{def}}{=} \|D |T(s)\rangle\|^2 = \|D^2 |\Psi(s)\rangle\|^2, \quad (6)$$

where $D \stackrel{\text{def}}{=} P^{(\Psi)} d/ds = (I - |\Psi\rangle \langle \Psi|) d/ds$ with $D |T(s)\rangle \stackrel{\text{def}}{=} P^{(\Psi)} |T'(s)\rangle = |\tilde{N}_*(s)\rangle$ representing the covariant derivative [21–23]. In this paper, we choose to use $|\tilde{N}_*(s)\rangle$ to express κ_{AC}^2 when we wish to avoid cumbersome expressions needed to define the covariant derivative D and the projection operator $P^{(\Psi)}$. From Eq. (6), we note that the curvature coefficient $\kappa_{\text{AC}}^2(s)$ is equal to the magnitude squared of the second covariant derivative of the state vector $|\Psi(s)\rangle$ that delineates the quantum Schrödinger trajectory in projective Hilbert space. For clarity, we emphasize that $|\tilde{N}_*(s)\rangle$ is a vector that is neither orthogonal to the vector $|T(s)\rangle$ nor normalized to one. Instead, despite not being properly normalized, $|\tilde{N}(s)\rangle \stackrel{\text{def}}{=} P^{(T)} P^{(\Psi)} |T'(s)\rangle$ is orthogonal to $|T(s)\rangle$. Finally, $|N(s)\rangle \stackrel{\text{def}}{=} |\tilde{N}(s)\rangle / \sqrt{\langle \tilde{N}(s) | \tilde{N}(s) \rangle}$ describes a normalized vector that is also orthogonal to $|T(s)\rangle$. In conclusion, $\{|\Psi(s)\rangle, |T(s)\rangle, |N(s)\rangle\}$ represents the set of three orthonormal vectors required to characterize the curvature of a quantum evolution. Observe that we focus our attention on the three-dimensional complex subspace spanned by $\{|\Psi(s)\rangle, |T(s)\rangle, |N(s)\rangle\}$, although \mathcal{H}_N can have arbitrary dimension N as a complex space. Nevertheless, our choice is consistent with the classical geometric perspective where the curvature and torsion coefficients can be viewed as the lowest and second-lowest, respectively, members of a family of generalized curvature functions [24]. In particular, for curves in higher-dimensional spaces, this well grounded geometric viewpoint requires a set of m orthonormal vectors in order to create $(m-1)$ -generalized curvature functions [24].

The explicit calculation of the time-dependent curvature coefficient $\kappa_{\text{AC}}^2(s)$ in Eqs. (6) based on the projection operators formalism is usually problematic. The challenge is due to the fact that, similarly to the classical case of space curves in \mathbb{R}^3 [7], there are essentially two drawbacks during the reparametrization of a quantum curve by its arc length s . First, we may not be able to calculate in closed form $s(t)$ in Eq. (3). Second, even if we are able to get $s = s(t)$, we may be unable to invert this relation and, thus, arrive at $t = t(s)$ needed to express $|\Psi(s)\rangle \stackrel{\text{def}}{=} |\Psi(t(s))\rangle$. To bypass these hurdles, we can recast $\kappa_{\text{AC}}^2(s)$ in Eq. (6) by means of expectation values taken with respect to the state $|\Psi(t)\rangle$ (or, alternatively, with respect to $|\psi(t)\rangle$) that can be calculated with no need of the relation $t = t(s)$ [15, 16]. For simplicity, we shall make no explicit reference to the s -dependence of the various operators and expectation values in the following discussion. For example, $\Delta h(s)$ will be written as Δh . After some algebraic manipulations, we obtain

$$|\tilde{N}_*\rangle = - \left\{ \left[(\Delta h)^2 - \langle (\Delta h)^2 \rangle \right] + i [\Delta h' - \langle \Delta h' \rangle] \right\} |\Psi\rangle, \quad (7)$$

where $\Delta h' = \partial_s (\Delta h) = [\partial_t (\Delta h)]/v(t)$. To evaluate $\kappa_{\text{AC}}^2(s) \stackrel{\text{def}}{=} \langle \tilde{N}_*(s) | \tilde{N}_*(s) \rangle$, it is useful to bring in the Hermitian operator $\hat{\alpha}_1 \stackrel{\text{def}}{=} (\Delta h)^2 - \langle (\Delta h)^2 \rangle$ and the anti-Hermitian operator $\hat{\beta}_1 \stackrel{\text{def}}{=} i[\Delta h' - \langle \Delta h' \rangle]$, where $\hat{\beta}_1^\dagger = -\hat{\beta}_1$. Then,

$|\tilde{N}_*\rangle = -(\hat{\alpha}_1 + \hat{\beta}_1)|\Psi\rangle$ and $\langle\tilde{N}_*(s)|\tilde{N}_*(s)\rangle$ is equal to $\langle\hat{\alpha}_1^2\rangle - \langle\hat{\beta}_1^2\rangle + \langle[\hat{\alpha}_1, \hat{\beta}_1]\rangle$, where $[\hat{\alpha}_1, \hat{\beta}_1] \stackrel{\text{def}}{=} \hat{\alpha}_1\hat{\beta}_1 - \hat{\beta}_1\hat{\alpha}_1$ denotes the quantum commutator of $\hat{\alpha}_1$ and $\hat{\beta}_1$. Observe that the expectation value $\langle[\hat{\alpha}_1, \hat{\beta}_1]\rangle$ is a real number since $[\hat{\alpha}_1, \hat{\beta}_1]$ is a Hermitian operator. This is a consequence of the fact that $\hat{\alpha}_1$ and $\hat{\beta}_1$ are Hermitian and anti-Hermitian operators, respectively. Employing the definitions of $\hat{\alpha}_1$ and $\hat{\beta}_1$, we get $\langle\hat{\alpha}_1^2\rangle = \langle(\Delta h)^4\rangle - \langle(\Delta h)^2\rangle^2$, $\langle\hat{\beta}_1^2\rangle = -\langle(\Delta h')^2\rangle$, and $\langle[\hat{\alpha}_1, \hat{\beta}_1]\rangle = i\langle[(\Delta h)^2, \Delta h']\rangle$. Note that, since $[(\Delta h)^2, \Delta h']$ is an anti-Hermitian operator, $\langle[(\Delta h)^2, \Delta h']\rangle$ is purely imaginary. For completeness, we stress that $[(\Delta h)^2, \Delta h']$ is not usually a null operator. Indeed, $[(\Delta h)^2, \Delta h'] = \Delta h[\Delta h, \Delta h'] + [\Delta h, \Delta h']\Delta h$ where $[\Delta h, \Delta h'] = [\mathbf{H}, \mathbf{H}']$. Then, limiting our attention to nonstationary qubit Hamiltonians of the form $\mathbf{H}(s) \stackrel{\text{def}}{=} \mathbf{h}(s) \cdot \boldsymbol{\sigma}$, the commutator $[\mathbf{H}, \mathbf{H}'] = 2i(\mathbf{h} \times \mathbf{h}') \cdot \boldsymbol{\sigma}$ can be nonzero since the vectors \mathbf{h} and \mathbf{h}' are not generally collinear. Clearly, $\boldsymbol{\sigma}$ denotes the vector operator whose components are specified by the usual Pauli operators σ_x, σ_y , and σ_z . Finally, a computationally convenient expression for the curvature coefficient $\kappa_{\text{AC}}^2(s)$ in Eq. (6) in an arbitrary nonstationary setting reduces to

$$\kappa_{\text{AC}}^2(s) = \langle(\Delta h)^4\rangle - \langle(\Delta h)^2\rangle^2 + \left[\langle(\Delta h')^2\rangle - \langle\Delta h'\rangle^2\right] + i\langle[(\Delta h)^2, \Delta h']\rangle. \quad (8)$$

From Eq. (8), we note that when the Hamiltonian \mathbf{H} is constant, $\Delta h'$ becomes the null operator and we recover the stationary limit $\langle(\Delta h)^4\rangle - \langle(\Delta h)^2\rangle^2$ of $\kappa_{\text{AC}}^2(s)$ [15].

The expression of $\kappa_{\text{AC}}^2(s)$ in Eq. (8) is obtained via an approach that relies upon the calculation of expectation values which, in turn, require the knowledge of the state vector $|\psi(t)\rangle$ governed by the time-dependent Schrödinger's evolution equation. As argued in Ref. [16], such expectation-values approach offers an insightful statistical interpretation for $\kappa_{\text{AC}}^2(s)$. At the same time, however, it is devoid of a clear geometrical interpretation. Motivated by this deficiency and focusing on nonstationary Hamiltonians and two-level quantum systems, it is possible to find a closed-form expression for the curvature coefficient for a curve mapped out by a single-qubit quantum state that evolves under an arbitrary nonstationary Hamiltonian. The curvature coefficient κ_{AC}^2 can be expressed completely in terms of exclusively two real three-dimensional vectors with a transparent geometric significance. Specifically, the two vectors are the Bloch vector $\mathbf{a}(t)$ and the magnetic field vector $\mathbf{h}(t)$. While the former vector emerges from the density operator $\rho(t) = |\psi(t)\rangle\langle\psi(t)| \stackrel{\text{def}}{=} [I + \mathbf{a}(t) \cdot \boldsymbol{\sigma}]/2$, the latter specifies the nonstationary Hamiltonian $\mathbf{H}(t) \stackrel{\text{def}}{=} \mathbf{h}(t) \cdot \boldsymbol{\sigma}$. Following the detailed analysis in Ref. [16], we get

$$\kappa_{\text{AC}}^2(\mathbf{a}, \mathbf{h}) = 4 \frac{(\mathbf{a} \cdot \mathbf{h})^2}{\mathbf{h}^2 - (\mathbf{a} \cdot \mathbf{h})^2} + \frac{\left[\mathbf{h}^2\dot{\mathbf{h}}^2 - (\mathbf{h} \cdot \dot{\mathbf{h}})^2\right] - \left[(\mathbf{a} \cdot \dot{\mathbf{h}})\mathbf{h} - (\mathbf{a} \cdot \mathbf{h})\dot{\mathbf{h}}\right]^2}{\left[\mathbf{h}^2 - (\mathbf{a} \cdot \mathbf{h})^2\right]^3} + 4 \frac{(\mathbf{a} \cdot \mathbf{h}) \left[\mathbf{a} \cdot (\mathbf{h} \times \dot{\mathbf{h}})\right]}{\left[\mathbf{h}^2 - (\mathbf{a} \cdot \mathbf{h})^2\right]^2}. \quad (9)$$

The expression of κ_{AC}^2 in Eq. (9) is very useful from a computational standpoint for qubit systems and, at the same time, offers a clear geometric interpretation of the curvature of a quantum evolution in terms of the (normalized unitless) Bloch vector \mathbf{a} and the (generally unnormalized, with $[\mathbf{h}]_{\text{MKSA}} = \text{joules} = \text{sec}^{-1}$ when setting $\hbar = 1$) magnetic field vector \mathbf{h} .

Having introduced the curvature coefficient $\kappa_{\text{AC}}^2(\mathbf{a}, \mathbf{h})$ in Eq. (9), we can finally introduce the time-dependent Hamiltonian $\mathbf{H}(t) = \mathbf{h}(t) \cdot \boldsymbol{\sigma}$ in what follows.

III. THE NONSTATIONARY HAMILTONIAN

In this section, we specify the dynamics governed by a two-parameter nonstationary Hamiltonian with unit speed efficiency.

A. Preliminaries

In Ref. [18], Uzdin and collaborators introduced suitable families of time-dependent Hamiltonians capable of producing predefined trajectories, not necessarily geodesic paths, with minimal waste of energetic resources. In particular, the condition of minimal waste of energetic resources is achieved when no energy is wasted on parts of the Hamiltonian that do not actively drive the system. In other words, all the available energy quantified in terms of the spectral norm of the Hamiltonian $\|\mathbf{H}\|_{\text{SP}}$ is converted into the speed of evolution of the system quantified by the

energy uncertainty ΔE , $v_{\mathbf{H}}(t) \stackrel{\text{def}}{=} (\gamma/\hbar)\Delta E(t)$. Observe that γ is an arbitrary positive constant whose chosen value depends on how the Fubini-Study metric is defined. For instance, while $\gamma = 1$ in Ref. [18], $\gamma = 2$ in Ref. [14]. More specifically, the so-called Uzdin's speed efficiency $\eta_{\text{SE}} = \eta_{\text{SE}}(t)$ is defined as [18]

$$\eta_{\text{SE}} \stackrel{\text{def}}{=} \frac{\Delta H_{\rho}}{\|\mathbf{H}\|_{\text{SP}}} = \frac{\sqrt{\text{tr}(\rho \mathbf{H}^2) - [\text{tr}(\rho \mathbf{H})]^2}}{\max[\sqrt{\text{eig}(\mathbf{H}^{\dagger} \mathbf{H})}]}, \quad (10)$$

where $\|\mathbf{H}\|_{\text{SP}} \stackrel{\text{def}}{=} \max[\sqrt{\text{eig}(\mathbf{H}^{\dagger} \mathbf{H})}]$ is the so-called spectral norm of the Hamiltonian operator \mathbf{H} and ρ is the density operator that describes the system. The spectral norm measures the size of bounded linear operators and is defined as the square root of the maximum eigenvalue of the operator $\mathbf{H}^{\dagger} \mathbf{H}$, with \mathbf{H}^{\dagger} being the Hermitian adjoint of \mathbf{H} . In what follows, we focus on qubit systems. Then, after recasting the generally time-dependent Hamiltonian in Eq. (10) as $\mathbf{H}(t) = h_0(t)\mathbf{I} + \mathbf{h}(t) \cdot \boldsymbol{\sigma}$, we note that η_{SE} in Eq. (10) can be formally recast as

$$\eta_{\text{SE}} = \frac{\sqrt{\mathbf{h} \cdot \mathbf{h} - (\mathbf{a} \cdot \mathbf{h})^2}}{|h_0| + \sqrt{\mathbf{h} \cdot \mathbf{h}}}, \quad (11)$$

with $\mathbf{a} = \mathbf{a}(t)$ being the instantaneous unit Bloch vector that specifies the qubit state of the system, and

$$\text{eig}(\mathbf{H}^{\dagger} \mathbf{H}) = \left\{ \lambda_{\mathbf{H}^{\dagger} \mathbf{H}}^{(+)} \stackrel{\text{def}}{=} (h_0 + \sqrt{\mathbf{h} \cdot \mathbf{h}})^2, \lambda_{\mathbf{H}^{\dagger} \mathbf{H}}^{(-)} \stackrel{\text{def}}{=} (h_0 - \sqrt{\mathbf{h} \cdot \mathbf{h}})^2 \right\}. \quad (12)$$

For completeness, observe that $\eta_{\text{SE}} = \eta_{\text{SE}}(t) \in [0, 1]$ is a local measure of efficiency for the quantum system. Furthermore, given that the eigenvalues of $\mathbf{H}(t) = h_0(t)\mathbf{I} + \mathbf{h}(t) \cdot \boldsymbol{\sigma}$ are given by $E_{\pm} \stackrel{\text{def}}{=} h_0 \pm \sqrt{\mathbf{h} \cdot \mathbf{h}}$, we have that $h_0 = (E_+ + E_-)/2$ is the average of the two energy levels. The quantity $\sqrt{\mathbf{h} \cdot \mathbf{h}} = (E_+ - E_-)/2$, instead, is proportional to the energy splitting between the two energy levels E_{\pm} . Finally, for a traceless nonstationary Hamiltonian $\mathbf{H}(t) = \mathbf{h}(t) \cdot \boldsymbol{\sigma}$, with $\mathbf{a}(t) \cdot \mathbf{h}(t) = 0$ for any instant t , $\eta_{\text{SE}}(t) = 1$ and the quantum evolution occurs with no waste of energetic resources.

What is the most general Hermitian nonstationary qubit Hamiltonian $\mathbf{H}(t)$ proposed in Ref. [18]? The Hamiltonian $\mathbf{H}(t)$ is constructed in such a manner that it generates the same motion $\pi(|\psi(t)\rangle)$ in the complex projective Hilbert space $\mathbb{C}P^1$ (or, equivalently, on the Bloch sphere $S^2 \cong \mathbb{C}P^1$) as $|\psi(t)\rangle$, where the projection operator π is such that $\pi: \mathcal{H}_2^1 \ni |\psi(t)\rangle \mapsto \pi(|\psi(t)\rangle) \in \mathbb{C}P^1$. In general, it can be shown that $\mathbf{H}(t)$ can be written as [18]

$$\mathbf{H}(t) = i|\partial_t m(t)\rangle \langle m(t)| - i|m(t)\rangle \langle \partial_t m(t)|, \quad (13)$$

where, for simplicity of notation, we can set $|m(t)\rangle = |m\rangle$ and $|\partial_t m(t)\rangle = |\partial_t m\rangle = \partial_t |m\rangle = |\dot{m}\rangle$. The state $|m\rangle$ is such that $\pi(|m(t)\rangle) = \pi(|\psi(t)\rangle)$, $i\partial_t |m(t)\rangle = \mathbf{H}(t)|m(t)\rangle$, and $\eta_{\text{SE}}(t) = 1$. The requirement that $\pi(|m(t)\rangle) = \pi(|\psi(t)\rangle)$ implies that $|m(t)\rangle = c(t)|\psi(t)\rangle$ for some complex function $c(t)$. Imposing that $\langle m|m\rangle = 1$, we get $|c(t)| = 1$. Therefore, $c(t) = e^{i\phi(t)}$ for some real function $\phi(t)$. Then, imposing the parallel transport condition $\langle m|\dot{m}\rangle = \langle \dot{m}|m\rangle = 0$, the phase $\phi(t)$ becomes equal to $i \int \langle \psi|\dot{\psi}\rangle dt$. Therefore, $|m(t)\rangle = \exp(-\int_0^t \langle \psi(t')|\partial_{t'} \psi(t')\rangle dt') |\psi(t)\rangle$. Observe that $|m(t)\rangle$ is the same as the parallel transported unit state vector $|\Psi(t)\rangle$ introduced in Eq. (2). However, in what follows, we keep the original notation employed in Ref. [18] and use $|m(t)\rangle$ instead of $|\Psi(t)\rangle$. Note that $\mathbf{H}(t)$ in Eq. (13) is traceless by construction since it possesses only off-diagonal elements in the orthogonal basis $\{|m\rangle, |\partial_t m\rangle\}$. Furthermore, the condition $i\partial_t |m(t)\rangle = \mathbf{H}(t)|m(t)\rangle$ implies that $|m(t)\rangle$ satisfies the Schrödinger evolution equation. Finally, the relation $\eta_{\text{SE}}(t) = 1$ signifies that $\mathbf{H}(t)$ drives $|m(t)\rangle$ with maximal speed with no waste of energy resources.

Having presented some basic preliminary material on Uzdin's work in Ref. [18], we can now introduce our proposed time-dependent unit speed efficiency Hamiltonian.

B. The Hamiltonian

In what follows, we aim to construct a time-dependent qubit Hamiltonian with 100% evolution speed that drives the quantum system with maximal speed efficiency (i.e., $\eta_{\text{SE}} = 1$, with η_{SE} in Eq. (10)) along a non-geodesic path (i.e., $0 \leq \eta_{\text{GE}} < 1$, with η_{GE} in Eq. (19)) on the Bloch sphere. Therefore, we expect the curvature $\kappa_{\text{AC}}^2(t)$ of the quantum evolution to be nonvanishing and, in principle, to exhibit a nonconstant temporal behavior.

We begin by considering a unit quantum state given by $|\psi(t)\rangle = \cos(\omega_0 t)|0\rangle + e^{i\nu_0 t} \sin(\omega_0 t)|1\rangle$, with ν_0 and ω_0 being the two essential real positive parameters that can be tuned when studying the quantum evolution. Recall that

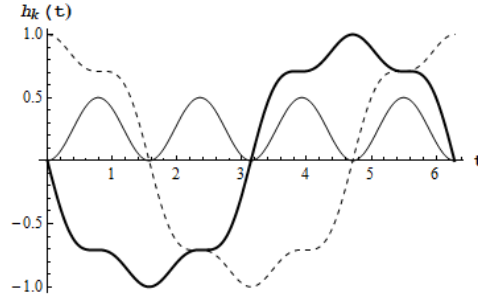


FIG. 1: Visualization of the temporal behavior of the magnetic field components $\{h_k\}_{1 \leq k \leq 3}$ with $h_1 = h_x$ (thick solid), $h_2 = h_y$ (dashed), and $h_3 = h_z$ (thin solid). In the plot, we set $\omega_0 = \nu_0 = 1$. Note that, in this case, $h_y(t) = h_x(t - \pi/2)$. Physical units are selected so that $\hbar = 1$.

in terms of the polar and azimuthal angles $\theta(t)$ and $\varphi(t)$, respectively, an arbitrary state on the Bloch sphere can be recast as $|\psi(t)\rangle = |\psi(\theta(t), \varphi(t))\rangle = \cos[\theta(t)/2]|0\rangle + e^{i\varphi(t)} \sin[\theta(t)/2]|1\rangle$. Therefore, we have $\omega_0 t = \theta(t)/2$ and $\nu_0 t = \varphi(t)$, that is, $\omega_0 = \dot{\theta}/2$ and $\nu_0 = \dot{\varphi}$. Since $\langle \psi(t) | \dot{\psi}(t) \rangle = i\nu_0 \sin^2(\omega_0 t) \neq 0$, $|\psi(t)\rangle$ is not parallel transported. From the state $|\psi(t)\rangle$, we consider the state $|m(t)\rangle \stackrel{\text{def}}{=} e^{-i\phi(t)} |\psi(t)\rangle$ with the phase $\phi(t)$ such that $\langle m(t) | \dot{m}(t) \rangle = 0$. A simple calculation implies that $\langle m(t) | \dot{m}(t) \rangle = 0$ if and only if $-i\dot{\phi} + \langle \psi(t) | \dot{\psi}(t) \rangle = 0$, that is $\dot{\phi} = -i \langle \psi(t) | \dot{\psi}(t) \rangle$. Setting $\phi(0) = 0$, the temporal behavior of the phase $\phi(t)$ is given by

$$\phi(t) = \frac{\nu_0}{4\omega_0} [2\omega_0 t - \sin(2\omega_0 t)]. \quad (14)$$

Furthermore, using Eq. (14), the parallel transported unit state $|m(t)\rangle$ becomes

$$|m(t)\rangle = e^{-i\frac{\nu_0}{4\omega_0} [2\omega_0 t - \sin(2\omega_0 t)]} [\cos(\omega_0 t) |0\rangle + e^{i\nu_0 t} \sin(\omega_0 t) |1\rangle]. \quad (15)$$

Then, setting the matrix representation of the Hamiltonian $H(t) = i(|\dot{m}\rangle \langle m| - |m\rangle \langle \dot{m}|)$ in the orthogonal basis $\{|m\rangle, |\dot{m}\rangle\}$ equal to $H(t) = h_0(t) \mathbf{I} + \mathbf{h}(t) \cdot \boldsymbol{\sigma}$, with $|m\rangle$ in Eq. (15), and, in addition, writing $\rho(t) = |m(t)\rangle \langle m(t)| = (1/2) [\mathbf{I} + \mathbf{a}(t) \cdot \boldsymbol{\sigma}]$, we obtain that the Bloch vector $\mathbf{a}(t)$ and the magnetic field vector $\mathbf{h}(t)$ are given by

$$\mathbf{a}(t) \stackrel{\text{def}}{=} \begin{pmatrix} \sin(\theta) \cos(\varphi) \\ \sin(\theta) \sin(\varphi) \\ \cos(\theta) \end{pmatrix} = \begin{pmatrix} \sin(2\omega_0 t) \cos(\nu_0 t) \\ \sin(\nu_0 t) \sin(2\omega_0 t) \\ \cos(2\omega_0 t) \end{pmatrix}, \quad (16)$$

and,

$$\mathbf{h}(t) = \begin{pmatrix} -\frac{\dot{\varphi}}{2} \cos(\theta) \sin(\theta) \cos(\varphi) - \frac{\dot{\theta}}{2} \sin(\varphi) \\ -\frac{\dot{\varphi}}{2} \cos(\theta) \sin(\theta) \sin(\varphi) + \frac{\dot{\theta}}{2} \cos(\varphi) \\ \frac{\dot{\varphi}}{2} \sin^2(\theta) \end{pmatrix} = \begin{pmatrix} -\frac{\nu_0}{2} \cos(2\omega_0 t) \sin(2\omega_0 t) \cos(\nu_0 t) - \omega_0 \sin(\nu_0 t) \\ -\frac{\nu_0}{2} \cos(2\omega_0 t) \sin(2\omega_0 t) \sin(\nu_0 t) + \omega_0 \cos(\nu_0 t) \\ \frac{\nu_0}{2} \sin^2(2\omega_0 t) \end{pmatrix}, \quad (17)$$

respectively, with $h_0(t) = 0$. The temporal behavior of the Cartesian components of the magnetic field vector $\mathbf{h} = \mathbf{h}_\perp + \mathbf{h}_\parallel = [h_x \hat{x} + h_y \hat{y}] + h_z \hat{z}$ is displayed in Fig. 1. As a consistency check, we verified that the two real three-dimensional vectors $\mathbf{a}(t)$ and $\mathbf{h}(t)$ in Eqs. (16) and (17), respectively, verify the relation $\dot{\mathbf{a}}(t) = 2\mathbf{h}(t) \times \mathbf{a}(t)$ as correctly expected (for details, see Appendix A). In Fig. 2, we illustrate the (nongeodesic) evolution path on the Bloch sphere that correspond to the Bloch vector $\mathbf{a}(t)$ in Eq. (16) and generated by the nonstationary Hamiltonian $H(t) = \mathbf{h}(t) \cdot \boldsymbol{\sigma}$ with $\mathbf{h}(t)$ in Eq. (17).

We are now ready to calculate the curvature coefficient $\kappa_{\text{AC}}^2(t)$ of the quantum evolution which drives $|m(t)\rangle$ in Eq. (15) under the nonstationary Hamiltonian $H(t) = \mathbf{h}(t) \cdot \boldsymbol{\sigma}$, with $\mathbf{h}(t)$ in Eq. (17) and with no waste of energy since $\eta_{\text{SE}}(t) = \sqrt{\langle \dot{m}(t) | \dot{m}(t) \rangle} / \sqrt{\langle m(t) | \dot{m}(t) \rangle}$ is constantly equal to one.

IV. QUANTUM EVOLUTION

Before calculating the curvature $\kappa_{\text{AC}}^2(t)$, we wish to study additional aspects of the quantum evolution so that we can gain a clearer physical interpretation of its curvature.

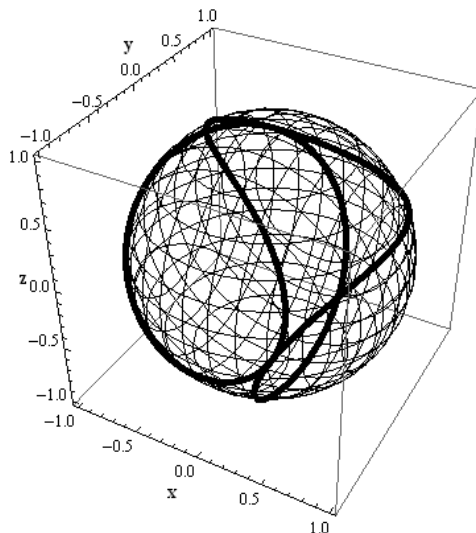


FIG. 2: Illustrative depiction of nongeodesic evolution paths (solid thick) on the Bloch sphere generated by the nonstationary Hamiltonian considered in the paper. For simplicity, we set here $\nu_0 = \omega_0 = 1$ and $0 \leq t \leq 20$. Physical units are chosen using $\hbar = 1$.

Geodesic efficiency. We begin by observing that the quantum evolution is nongeodesic. Indeed, consider the evolution between two orthogonal quantum states $|m(t_A)\rangle$ and $|m(t_B)\rangle$ with $t_A = 0$ and $t_B = \pi/(2\omega_0)$. The energy dispersion $\Delta E(t) \stackrel{\text{def}}{=} \sqrt{\text{tr}(\rho H^2) - [\text{tr}(\rho H)]^2} = \sqrt{\langle \dot{m}(t) | \dot{m}(t) \rangle}$ is given by,

$$\Delta E(t; \omega_0, \nu_0) = \omega_0 \sqrt{1 + \frac{1}{4} \left(\frac{\nu_0}{\omega_0} \right)^2 \sin^2(2\omega_0 t)}. \quad (18)$$

Then, the Anandan-Aharonov geodesic efficiency η_{GE} defined as [19, 20]

$$\eta_{\text{GE}} \stackrel{\text{def}}{=} \frac{2 \arccos[|\langle m(t_A) | m(t_B) \rangle|]}{2 \int_{t_A}^{t_B} \frac{\Delta E(t')}{\hbar} dt'}, \quad (19)$$

becomes

$$\eta_{\text{GE}}(\omega_0, \nu_0) = \frac{\pi}{2} \frac{1}{E\left(-\frac{1}{4} \left(\frac{\nu_0}{\omega_0} \right)^2\right)} < 1, \quad (20)$$

where $E(m)$ in Eq. (20) is the complete elliptic integral of the second kind with parameter m [25]. For instance, setting $\nu_0 = \omega_0 = 1$, $E(-1/4) \simeq 1.66 > \pi/2$. Since $\eta_{\text{GE}} < 1$ from Eq. (20), we expect that $\kappa_{\text{AC}}^2(t) \neq 0$. Interestingly, for $\nu_0 = 0$, $E(0) = \pi/2$ and η_{GE} in Eq. (20) equals one. For this choice of parameters, the state $|m(t)\rangle = \cos(\omega_0 t) |0\rangle + \sin(\omega_0 t) |1\rangle$ describes a great circle on the Bloch sphere. Thus, the quantum evolution becomes geodesic.

Speed. The speed of quantum evolution in projective Hilbert space is given by $v_{\text{H}}(t)$ with

$$v_{\text{H}}^2(t) \stackrel{\text{def}}{=} [\Delta E(t)]^2 = \langle \dot{m}(t) | \dot{m}(t) \rangle = \omega_0^2 + \frac{\nu_0^2}{4} \sin^2(2\omega_0 t). \quad (21)$$

Therefore, $v_{\text{H}}(t)$ equals

$$v_{\text{H}}(t; \omega_0, \nu_0) = \omega_0 \sqrt{1 + \frac{1}{4} \left(\frac{\nu_0}{\omega_0} \right)^2 \sin^2(2\omega_0 t)}. \quad (22)$$

From Eq. (22), we observe that $\bar{v}_{\text{H}} \stackrel{\text{def}}{=} \max_t [v_{\text{H}}(t)] = \omega_0 \sqrt{1 + (1/4)(\nu_0/\omega_0)^2}$ is reached at $t_{\text{max}}^v \stackrel{\text{def}}{=} \pi/(4\omega_0) + [\pi/(2\omega_0)]n$, with $n \in \mathbb{Z}$. In particular, the instances t_{max}^v are obtained by noting that $\sin^2(2\omega_0 t) = [1 - \cos(4\omega_0 t)]/2 =$

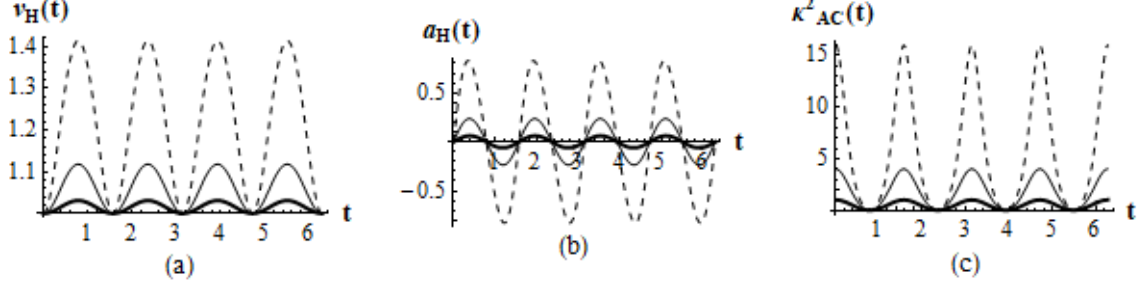


FIG. 3: Graphical visualization of the quantum evolution speed $v_H(t)$ (a), the acceleration of the quantum evolution $a_H(t)$ (b) and, finally, the curvature coefficient $\kappa_{AC}^2(t)$ (c) versus time t with $0 \leq t \leq 2\pi$. Dashed, solid thin, and solid thick lines are specified by the conditions $\nu_0 = 2\omega_0$, $\nu_0 = \omega_0$, and $\nu_0 = \omega_0/2$, respectively. In all cases, we set $\omega_0 = 1$. Physical units are chosen so that $\hbar = 1$.

1 iff $4\omega_0 t_{\max}^v = \pi + 2\pi n$. Similarly, $\underline{v}_H \stackrel{\text{def}}{=} \min_t [v_H(t)] = \omega_0$ is obtained when $4\omega_0 t_{\min}^v = 2\pi n$, that is for $t_{\min}^v \stackrel{\text{def}}{=} [\pi/(2\omega_0)]n$, with $n \in \mathbb{Z}$. Finally, observe that $v_H(t; \omega_0, \nu_0)$ in Eq. (22) is periodic of $T \stackrel{\text{def}}{=} \pi/(2\omega_0)$.

Acceleration. The acceleration $a_H(t)$ of the quantum evolution is the rate of change in time of the magnitude of the speed of quantum evolution $v_H(t)$. Therefore, it is given by $a_H(t) \stackrel{\text{def}}{=} dv_H(t)/dt$ and, in our case, becomes

$$a_H(t; \omega_0, \nu_0) = \frac{1}{4} \frac{\nu_0^2 \sin(4\omega_0 t)}{\sqrt{1 + \frac{1}{4} \left(\frac{\nu_0}{\omega_0}\right)^2 \sin^2(2\omega_0 t)}}. \quad (23)$$

Following the reasoning provided for the speed of quantum evolution, we note that $\bar{a}_H \stackrel{\text{def}}{=} \max_t [a_H(t)] = (\nu_0^2/4) \left[1 + \frac{1}{8} \left(\frac{\nu_0}{\omega_0}\right)^2\right]^{-1/2}$ at $t_{\max}^a = \pi/(8\omega_0) + [\pi/(2\omega_0)]n$, with $n \in \mathbb{Z}$. Furthermore, $\underline{a}_H \stackrel{\text{def}}{=} \min_t [a_H(t)] = -\bar{a}_H$ at $t_{\min}^a = 3\pi/(8\omega_0) + [\pi/(2\omega_0)]n$, with $n \in \mathbb{Z}$. Finally, notice that $a_H(t; \omega_0, \nu_0)$ in Eq. (23) is periodic of $T \stackrel{\text{def}}{=} \pi/(2\omega_0)$.

Magnetic field components. To illustrate how the parameters ω_0 and ν_0 are related to the non-static configuration of the magnetic field, we consider the ratio between the intensity of the magnetic field component along the z -axis (i.e., parallel to the quantization axis) and the intensity of the magnetic field component that lays in the xy -plane (i.e., transverse to the quantization axis). This consideration is reasonable. Indeed, for example, in typical experimental conditions for quantum-mechanical Rabi oscillations, the ratio between these two intensities is much greater than one [26–29]. Specifically, $\mathbf{h}(t)$ in Eq. (17) can be decomposed in a parallel component \mathbf{h}_{\parallel} along the z -axis and a transverse component \mathbf{h}_{\perp} that is perpendicular to the z -axis (i.e., a component in the xy -plane). Specifically, we can write $\mathbf{h} \stackrel{\text{def}}{=} \mathbf{h}_{\perp} + \mathbf{h}_{\parallel}$, with $\mathbf{h}_{\perp} \stackrel{\text{def}}{=} (\mathbf{h} \cdot \hat{x}) \hat{x} + (\mathbf{h} \cdot \hat{y}) \hat{y}$ and $\mathbf{h}_{\parallel} \stackrel{\text{def}}{=} (\mathbf{h} \cdot \hat{z}) \hat{z}$. In our case, we have $\mathbf{h}_{\perp}^2 = (\nu_0^2/16) \sin^2(4\omega_0 t) + \omega_0^2$ and $\mathbf{h}_{\parallel}^2 = (\nu_0^2/4) \sin^4(2\omega_0 t)$. Therefore, the ratio $\left(\frac{\mathbf{h}_{\parallel}^2}{\mathbf{h}_{\perp}^2}\right)(t; \omega_0, \nu_0)$ reduces to

$$\left(\frac{\mathbf{h}_{\parallel}^2}{\mathbf{h}_{\perp}^2}\right)(t; \omega_0, \nu_0) = 4 \frac{\sin^4(2\omega_0 t)}{\sin^2(4\omega_0 t) + 16 \left(\frac{\omega_0}{\nu_0}\right)^2}. \quad (24)$$

From Eq. (24), we observe that the local maxima of the ratio $\mathbf{h}_{\parallel}^2/\mathbf{h}_{\perp}^2$ are given by $(\mathbf{h}_{\parallel}^2/\mathbf{h}_{\perp}^2)_{\max} = (1/4)(\nu_0/\omega_0)^2$ and are reached at $\bar{t}_* = \pi/(4\omega_0) + [\pi/(2\omega_0)]n$, with $n \in \mathbb{Z}$. Moreover, the local minima of the ratio $\mathbf{h}_{\parallel}^2/\mathbf{h}_{\perp}^2$ are given by $(\mathbf{h}_{\parallel}^2/\mathbf{h}_{\perp}^2)_{\min} = 0$ and are reached at $\underline{t}_* = [\pi/(2\omega_0)]n$ with $n \in \mathbb{Z}$. Finally, observe that $\mathbf{h}_{\parallel}^2/\mathbf{h}_{\perp}^2$ in Eq. (24) is periodic of $T \stackrel{\text{def}}{=} \pi/(2\omega_0)$.

Curvature. We are now ready to calculate the curvature coefficient $\kappa_{AC}^2(t)$ of the quantum evolution which drives $|m(t)\rangle$ in Eq. (15) under the nonstationary Hamiltonian $H(t) = \mathbf{h}(t) \cdot \boldsymbol{\sigma}$, with $\mathbf{h}(t)$ in Eq. (17). Then, given $\mathbf{a}(t)$ in Eq. (16) and $\mathbf{h}(t)$ in Eq. (17), we note that $\mathbf{a} \cdot \mathbf{h} = 0$ and $\mathbf{a} \cdot \dot{\mathbf{h}} = 0$. For completeness, we remark that no tedious calculation is necessary to explain that $\mathbf{a} \cdot \dot{\mathbf{h}} = 0$ once one verifies that $\mathbf{a} \cdot \mathbf{h} = 0$. Indeed, exploiting the constraint

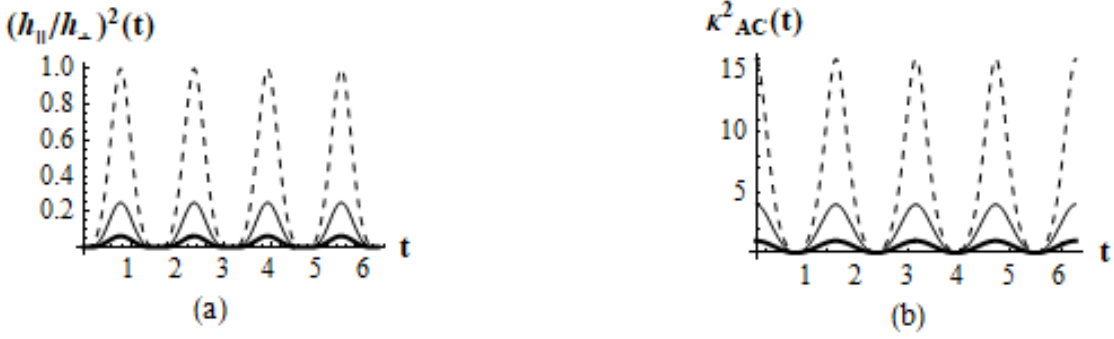


FIG. 4: Plots of the ratio squared between the parallel and the transverse magnetic field vector intensities $(h_{\parallel}/h_{\perp})^2(t)$ (a) and the curvature coefficient $\kappa_{\text{AC}}^2(t)$ (b) versus time t with $0 \leq t \leq 2\pi$. Dashed, solid thin, and solid thick lines are defined by the relations $\nu_0 = 2\omega_0$, $\nu_0 = \omega_0$, and $\nu_0 = \omega_0/2$, respectively. In all cases, we put $\omega_0 = 1$. Physical units are selected so that $\hbar = 1$.

equation $\dot{\mathbf{a}} = 2\mathbf{h} \times \mathbf{a}$ (for details, see Appendix A), $\mathbf{a} \cdot \dot{\mathbf{h}} = 0$ follows from elementary algebraic steps and simple geometric reasoning. Therefore, the curvature coefficient $\kappa_{\text{AC}}^2(\mathbf{a}, \mathbf{h})$ in Eq. (9) reduces to

$$\kappa_{\text{AC}}^2(\mathbf{a}, \mathbf{h}) = \frac{\mathbf{h}^2 \dot{\mathbf{h}}^2 - (\mathbf{h} \cdot \dot{\mathbf{h}})^2}{\mathbf{h}^6}, \quad (25)$$

that is, after some algebra, we get that

$$\kappa_{\text{AC}}^2(t; \omega_0, \nu_0) = \frac{\sin^2(4\omega_0 t) + 32(\frac{\omega_0}{\nu_0})^2 [1 + \cos(4\omega_0 t)]}{\left[\sin^2(2\omega_0 t) + 4(\frac{\omega_0}{\nu_0})^2 \right]^2} - 4(\frac{\omega_0}{\nu_0})^2 \frac{\sin^2(4\omega_0 t)}{\left[\sin^2(2\omega_0 t) + 4(\frac{\omega_0}{\nu_0})^2 \right]^3}. \quad (26)$$

It is worthwhile pointing out that, unlike what happens in quantum evolutions governed by stationary Hamiltonians [15], the condition $\mathbf{a} \cdot \mathbf{h} = 0$ is not sufficient for having a vanishing curvature coefficient. As a side remark, we stress that this condition becomes sufficient only if we add the additional assumption that the magnetic field vector does not change direction in time (i.e., if \mathbf{h} and $\dot{\mathbf{h}}$ are collinear). Unfortunately, as evident from Eq. (17), this is not the case in the problem being analyzed here. We emphasize that $(\kappa_{\text{AC}}^2)_{\text{max}} \stackrel{\text{def}}{=} \max_t [\kappa_{\text{AC}}^2(t)] = 4(\nu_0/\omega_0)^2$ at $t_{\text{max}}^{\kappa} = [\pi/(2\omega_0)]n$, with $n \in \mathbb{Z}$. Furthermore, $(\kappa_{\text{AC}}^2)_{\text{min}} \stackrel{\text{def}}{=} \min_t [\kappa_{\text{AC}}^2(t)] = 0$ at $t_{\text{min}}^{\kappa} = \pi/(4\omega_0) + [\pi/(2\omega_0)]n$, with $n \in \mathbb{Z}$. Interestingly, as ν_0 approaches zero, we correctly recover a geodesic quantum evolution with a vanishing curvature coefficient κ_{AC}^2 in Eq. (26). Finally, notice that $\kappa_{\text{AC}}^2(t; \omega_0, \nu_0)$ in Eq. (26) is periodic of $T \stackrel{\text{def}}{=} \pi/(2\omega_0)$. To the best of our knowledge, Eq. (26) is the first example of a closed form expression for the curvature coefficient of a quantum evolution specified by a two-parameter nonstationary (traceless) Hamiltonian for two-level quantum systems.

In what follows, we summarize a number of considerations on the temporal behaviors of $v_{\text{H}}(t)$ in Eq. (22), $a_{\text{H}}(t)$ in Eq. (23), $(\mathbf{h}_{\parallel}^2/\mathbf{h}_{\perp}^2)(t)$ in Eq. (24), and $\kappa_{\text{AC}}^2(t)$ in Eq. (26). First, each and everyone of these quantities displays a periodic oscillatory behavior characterized by a period $T \stackrel{\text{def}}{=} \pi/(2\omega_0)$. Second, the relation between the behaviors of $v_{\text{H}}(t)$ and $a_{\text{H}}(t) \stackrel{\text{def}}{=} dv_{\text{H}}(t)/dt$ is clear, since the acceleration $a_{\text{H}}(t)$ is the temporal rate of change of the speed $v_{\text{H}}(t)$ of the quantum evolution in projective Hilbert space. Third, whenever $v_{\text{H}}(t)$ decreases, $\kappa_{\text{AC}}^2(t)$ increases (and vice versa). In particular, whenever $v_{\text{H}}(t)$ reaches its maximum value (minimum value, respectively), the curvature coefficient $\kappa_{\text{AC}}^2(t)$ assumes its minimum value (maximum value, respectively). Fourth, the acceleration $a_{\text{H}}(t)$ vanishes whenever $\kappa_{\text{AC}}^2(t)$ reaches its local minima and maxima. Fifth, $v_{\text{H}}(t)$ and $(\mathbf{h}_{\parallel}^2/\mathbf{h}_{\perp}^2)(t)$ exhibit the same monotonic behavior. In particular, whenever $v_{\text{H}}(t)$ assumes its maximum value (minimum value, respectively), $(\mathbf{h}_{\parallel}^2/\mathbf{h}_{\perp}^2)(t)$ reaches its maximum value (minimum value, respectively). Finally, given the links between the pairs $(v_{\text{H}}(t), \kappa_{\text{AC}}^2(t))$ and $(v_{\text{H}}(t), (\mathbf{h}_{\parallel}^2/\mathbf{h}_{\perp}^2)(t))$, the comparative analysis between the temporal behaviors of $\kappa_{\text{AC}}^2(t)$ and $(\mathbf{h}_{\parallel}^2/\mathbf{h}_{\perp}^2)(t)$ becomes self-evident. Finally, while the plots of $v_{\text{H}}(t)$, $a_{\text{H}}(t)$, $\kappa_{\text{AC}}^2(t)$ as functions of time are illustrated in Fig. 3 for different choices of the two parameters ω_0 and ν_0 , the temporal behaviors of $(\mathbf{h}_{\parallel}^2/\mathbf{h}_{\perp}^2)(t)$ and $\kappa_{\text{AC}}^2(t)$ are displayed in Fig. 4.

We are now ready for our summary of results and final comments.

V. CONCLUDING REMARKS

In this paper, we discussed a first important example of an exact analytical expression of the curvature coefficient $\kappa_{\text{AC}}^2(t; \omega_0, \nu_0)$ (Eq. (26) and Fig. 1) of a quantum evolution for a two-level quantum system in a time-dependent magnetic field $\mathbf{h}(t)$ (Eq. (17)). Specifically, we investigated the dynamics generated by a two-parameter (i.e., ω_0 and ν_0 in Eq. (15)) nonstationary Hermitian Hamiltonian $H(t) = \mathbf{h}(t) \cdot \boldsymbol{\sigma}$ with unit speed efficiency η_{SE} (Eq. (11)). The two parameters ω_0 and ν_0 specify the constant temporal rates of change of the polar and azimuthal angles (i.e., $\omega_0 = \dot{\theta}/2$ and $\nu_0 = \dot{\varphi}$) employed in the Bloch sphere representation of the evolving pure state (with Bloch vector $\mathbf{a}(t)$ in Eq. (16) and in Fig. 2). To better grasp the physical significance of the curvature coefficient $\kappa_{\text{AC}}^2(t; \omega_0, \nu_0)$, showing that the quantum evolution is nongeodesic since the geodesic efficiency η_{GE} of the quantum evolution is strictly less than one (Eq. (20)) and tuning the two Hamiltonian parameters, we compared in Fig. 3 the temporal behavior of the curvature coefficient $\kappa_{\text{AC}}^2(t; \omega_0, \nu_0)$ with that of the speed $v_{\text{H}}(t)$ (22) and the acceleration $a_{\text{H}}(t)$ (23) of the evolution in projective Hilbert space. Furthermore, we compared in Fig. 4 the temporal profile of the curvature coefficient $\kappa_{\text{AC}}^2(t; \omega_0, \nu_0)$ with that of the square of the ratio $(\mathbf{h}_{\parallel}^2/\mathbf{h}_{\perp}^2)(t)$ between the parallel and transverse magnetic field intensities (Eq. (24)).

The primary conclusions to be drawn can be outlined as follows. First, unlike what happens in a stationary setting, the condition $\mathbf{a} \cdot \mathbf{h} = 0$ is neither necessary nor sufficient to get a quantum evolution with a vanishing curvature in the time-varying framework. Instead, when \mathbf{h} does not change in direction (i.e., if \mathbf{h} and $\dot{\mathbf{h}}$ are collinear) and $\mathbf{a} \cdot \mathbf{h} = 0$, the curvature vanishes. Second, the bending of quantum paths on the Bloch sphere does not need to happen with waste of energy resources (i.e., $\kappa_{\text{AC}}^2 \neq 0$ does not imply $\eta_{\text{SE}} < 1$). Third, no bending happens only with unit geodesic efficiency (i.e., $\kappa_{\text{AC}}^2 = 0$ only when $\eta_{\text{GE}} = 1$). More specifically, our notion of bending is defined in terms of our proposed curvature coefficient κ_{AC}^2 . For a geodesic motion on the Bloch sphere equipped with the Fubini-Study metric, κ_{AC}^2 vanishes and the geodesic efficiency η_{GE} equals one. Instead, the bending quantified by the Frenet-Serret curvature coefficient would be always present when lines are not straight (for example, consider a circle in the equatorial plane of a sphere in \mathbb{R}^3). Moreover, despite the fact that the bending phenomenon can emerge, in principle, from the (deterministic) evolution of an arbitrary quantum system in a pure state that evolves unitarily according to the Schrödinger equation, its quantification is intrinsically linked to the probabilistic nature of quantum theory. Indeed, for a discussion on how to express our curvature and the torsion coefficients of a quantum evolution in terms of statistical concepts, including kurtosis and skewness, we suggest Refs. [15, 16]. Fourth, regions of high (low) curvature coefficients κ_{AC}^2 are characterized by low (high) speed v_{H} of quantum evolutions. In particular, the acceleration a_{H} of quantum evolutions vanishes when the curvature coefficient κ_{AC}^2 achieves its local extrema (i.e., local minima and local maxima). Fifth, the curvature coefficient κ_{AC}^2 and the ratio squared between the parallel and transverse magnetic field intensities exhibit the same oscillatory behavior for the scenario being investigated here. In particular, high (low) curvature regions correspond to high (low) $\mathbf{h}_{\parallel}^2/\mathbf{h}_{\perp}^2$ ratios.

As pointed out in Ref. [14], the geometric concepts of curvature and torsion of quantum evolutions are interesting on their own rights. Unfortunately, these notions were only defined for stationary Hamiltonians in Ref. [14]. In recent years, being their applicability limited to time-independent Hamiltonian settings, these concepts have been successfully used to characterize geometric aspects of graph states in Ref. [30] and geometric features of unitary dynamical evolutions employed to solve combinatorial optimization problems with continuous-time quantum algorithms in Ref. [31]. Our geometric analysis, instead, paves the way to fully time-dependent curvature investigations of quantum evolutions that go beyond the very-short-time limits of the expectation values of suitable observable of the quantum systems being analyzed [31].

As mentioned in the Introduction, the notions of curvature and torsion of quantum evolutions have been remarkably reconstructed in an alternative fashion (with respect to Ref. [14]) in a time-independent setting in Ref. [15] and, most importantly, extended to a fully time-dependent setting in Ref. [16]. However, the illustrative single-qubit example discussing the concept of curvature in Ref. [16] was carried out in a numerical fashion. Furthermore, no discussion on the link between curvature and other quantum evolution quantifiers such as the speed efficiency, the geodesic efficiency, and the magnetic field parallel and transverse configurations was presented in Ref. [16]. In view of these considerations, despite the fact that our analytical investigation is limited to a two-level quantum system (and, in addition, to a particular time-varying magnetic field configuration) and its extension to higher-dimensional systems is expected to be nontrivial [16], we believe that our analysis constitutes a nontrivial piece of work that paves the way to geometric characterizations of more realistic quantum evolutions.

We remark that, modulo computational tediousness, the main difficulties that emerge when applying our approach to arbitrary nonstationary magnetic field configurations for two-level quantum systems arise from the complications in obtaining exact analytical solutions to the time-dependent Schrödinger equation [32–40]. Moreover, while the formula for κ_{AC}^2 is theoretically valid for any d -level quantum system that evolves under a nonstationary Hamiltonian,

our study was confined to systems with just two levels. In this more straightforward situation, the understanding and visual representation of Bloch vectors and Bloch spheres are straightforward, unlike in more complex, higher-dimensional situations. As we move from systems with just two levels to those with more dimensions, the clarity of these visualizations decreases. In fact, quantum theory exhibits unique characteristics in more complex systems, including the simplest yet non-trivial example with three levels, which are known as qutrits [41]. These peculiar quantum behaviors make it challenging to understand the geometric structure of quantum systems in higher dimensions [42, 43]. We recommend Ref. [44] for a comprehensive overview of how Bloch vectors are used to represent single-qubit, single-qutrit, and two-qubit systems, using matrices such as Pauli, Gell-Mann, and Dirac matrices, respectively.

Realistic evolutions are expected to occur in larger Hilbert spaces where the emergence of quantum entanglement and, in addition, the nature of the possibly time-dependent interactions among the various elements of the composite system can lead to a rather rich dynamical setting where geometric concepts like curvature and torsion can be a helpful investigative tool [30, 31]. Moreover, given the intriguing link between the concepts of complexity and efficiency of quantum evolutions [45–47] together with the connection between curvature and efficiencies mentioned here, we expect the concept of curvature to play a determinant role in determining the complexity of quantum-mechanical evolutions [48–54] as well.

To sum up, even though it has its present constraints, we truly believe that our research will encourage other researchers and set the stage for more in-depth studies on how geometry and quantum mechanics interact.

Acknowledgments

C.C. thanks Christian Corda for helpful remarks. Furthermore, the authors are grateful to anonymous referees for constructive comments leading to an improved version of the paper. Any opinions, findings and conclusions or recommendations expressed in this material are those of the author(s) and do not necessarily reflect the views of their home Institutions.

-
- [1] R. P. Feynman, F. Vernon, and R. W. Hellwarth, *Geometrical representation of the Schrödinger equation for solving maser problems*, J. Appl. Phys. **28**, 49 (1957).
 - [2] R. Dandoloff, R. Balakrishnan, and A. R. Bishop, *Two-level systems: Space curve formalism, Berry's phase and Gauss-Bonnet theorem*, J. Phys. A: Math. Gen. **25**, L1105 (1992).
 - [3] L. Carmel and A. Mann, *Geometrical approach to two-level Hamiltonians*, Phys. Rev. **A61**, 052113 (2000).
 - [4] R. Balakrishnan and R. Dandoloff, *Classical analogues of the Schrödinger and Heisenberg pictures in quantum mechanics using the Frenet frame of a space curve: An example*, Eur. J. Phys. **25**, 447 (2004).
 - [5] Z.-J. Ying, P. Gentile, J. P. Baltanas, D. Frustaglia, C. Ortix, and M. Cuoco, *Geometric driving of two-level quantum systems*, Phys. Rev. Research **2**, 023167 (2020).
 - [6] T. Salamone, M. Skjaerpe, H. G. Hugdal, M. Amundsen, and S. H. Jacobsen, *Interface probe for antiferromagnets using geometric curvature*, Phys. Rev. **B109**, 094508 (2024).
 - [7] R. Millman and G. Parker, *Elements of Differential Geometry*, Prentice Hall, NY (1977).
 - [8] E. Cartan, *Sur les varietes a connexion affine et la theorie de la relativite generalisee (premiere partie)*, Annales Scientifiques de l'Ecole Normale Supérieure **40**, 325 (1923).
 - [9] O. Consa, *Helical solenoid model of electron*, Progress in Physics **14**, 80 (2018).
 - [10] K. E. Ozen, F. S. Dundar, and M. Tosun, *An alternative approach to jerk in motion along a space curve with applications*, J. Theor. Appl. Mech. **57**, 435 (2019).
 - [11] K. E. Ozen, M. Guner, and M. Tosun, *A note on the acceleration and jerk in motion along a space curve*, An. St. Univ. Ovidius Const. **28**, 151 (2020).
 - [12] D. B. Brody and L. P. Hughston, *Geometry of quantum statistical inference*, Phys. Rev. Lett. **77**, 2851 (1996).
 - [13] D. C. Brody and Eva-Marie Graefe, *Information geometry of complex Hamiltonians and exceptional points*, Entropy **15**, 3361 (2013).
 - [14] H. P. Laba and V. M. Tkachuk, *Geometric characteristics of quantum evolution: Curvature and torsion*, Condensed Matter Physics **20**, 13003 (2017).
 - [15] P. M. Alsing and C. Cafaro, *From the classical Frenet–Serret apparatus to the curvature and torsion of quantum-mechanical evolutions. Part I. Stationary Hamiltonians*, Int. J. Geom. Methods Mod. Phys. **21**, 2450152 (2024).
 - [16] P. M. Alsing and C. Cafaro, *From the classical Frenet–Serret apparatus to the curvature and torsion of quantum-mechanical evolutions. Part II. Nonstationary Hamiltonians*, Int. J. Geom. Methods Mod. Phys. **21**, 2450151 (2024).
 - [17] P. M. Alsing and C. Cafaro, *Upper limit on the acceleration of a quantum evolution in projective Hilbert space*, Int. J. Geom. Methods Mod. Phys. **21**, 2440009 (2024).

- [18] R. Uzdin, U. Gunther, S. Rahav, and N. Moiseyev, *Time-dependent Hamiltonians with 100% evolution speed efficiency*, J. Phys. A: Math. Theor. **45**, 415304 (2012).
- [19] J. Anandan and Y. Aharonov, *Geometry of quantum evolution*, Phys. Rev. Lett. **65**, 1697 (1990).
- [20] C. Cafaro, S. Ray, and P. M. Alsing, *Geometric aspects of analog quantum search evolutions*, Phys. Rev. **A102**, 052607 (2020).
- [21] C. Cafaro and P. M. Alsing, *Qubit geodesics on the Bloch sphere from optimal-speed Hamiltonian evolutions*, Class. Quantum Grav. **40**, 115005 (2023).
- [22] J. Samuel and R. Bhandari, *General setting for Berry's phase*, Phys. Rev. Lett. **60**, 2339 (1988).
- [23] P. M. Alsing, C. Cafaro, O. Luongo, C. Lupo, S. Mancini, and H. Quevedo, *Comparing metrics for mixed quantum states: Sjöqvist and Bures*, Phys. Rev. **A107**, 052411 (2023).
- [24] J. Alvarez-Vizoso, R. Arn, M. Kirby, C. Peterson, and B. Draper, *Geometry of curves in \mathbb{R}^n from the local singular value decomposition*, Lin. Algebra Appl. **571**, 180 (2019).
- [25] I. S. Gradshteyn and I. M. Ryzhik, *Tables of Integrals, Series, and Products*, Academic Press (2000).
- [26] J. J. Sakurai, *Modern Quantum Mechanics*, Addison-Wesley Publishing Company, Inc. (1994).
- [27] I. I. Rabi, N. F. Ramsey, and J. Schwinger, *Use of rotating coordinates in magnetic resonance problems*, Rev. Mod. Phys. **26**, 167 (1954).
- [28] C. Cafaro and P. M. Alsing, *Continuous-time quantum search and time-dependent two-level quantum systems*, Int. J. Quantum Information **17**, 1950025 (2019).
- [29] C. Cafaro, S. Gassner, and P. M. Alsing, *Information geometric perspective on off-resonance effects in driven two-level quantum systems*, Quantum Reports **2**, 166 (2020).
- [30] Kh. P. Gnatenko, H. P. Laba, and V. M. Tkachuk, *Geometric properties of evolutionary graph states and their detection on a quantum computer*, Phys. Lett. **A452**, 128434 (2022).
- [31] R. J. Banks et al., *Continuous-time quantum walks for MAX-CUT are hot*, Quantum **8**, 1254 (2024).
- [32] L. Landau, *A theory of energy transfer. II*, Phys. Z. Sowjet **2**, 46 (1932).
- [33] C. Zener, *Non-adiabatic crossing of energy levels*, Proc. R. Soc. **A137**, 696 (1932).
- [34] I. I. Rabi, *Space quantization in a gyrating magnetic field*, Phys. Rev. **51**, 652 (1937).
- [35] E. Barnes and S. Das Sarma, *Analytically solvable driven time-dependent two-level quantum systems*, Phys. Rev. Lett. **109**, 060401 (2012).
- [36] E. Barnes, *Analytically solvable two-level quantum systems and Landau-Zener interferometry*, Phys. Rev. **A88**, 013818 (2013).
- [37] A. Messina and H. Nakazato, *Analytically solvable Hamiltonians for quantum two-level systems and their dynamics*, J. Phys. A: Math and Theor. **47**, 44302 (2014).
- [38] R. Grimaudo, A. S. Magalhaes de Castro, H. Nakazato, and A. Messina, *Classes of exactly solvable generalized semi-classical Rabi systems*, Annalen der Physik **530**, 1800198 (2018).
- [39] E. R. Loubenets and C. Kading, *Specifying the unitary evolution of a qudit for a general nonstationary Hamiltonian via the generalized Gell-Mann representation*, Entropy **22**, 521 (2020).
- [40] A. S. Magalhaes de Castro, R. Grimaudo, D. Valenti, A. Migliore, H. Nakazato, and A. Messina, *Analytically solvable Hamiltonian in invariant subspaces*, Eur. Phys. J. Plus **138**, 766 (2023).
- [41] P. Kurzynski, *Multi-Bloch vector representation of the qutrit*, Quantum Inf. Comp. **11**, 361 (2011).
- [42] J. Xie et al., *Observing geometry of quantum states in a three-level system*, Phys. Rev. Lett. **125**, 150401 (2020).
- [43] C. Eltschka, M. Huber, S. Morelli, and J. Siewert, *The shape of higher-dimensional state space: Bloch-ball analog for a qutrit*, Quantum **5**, 485 (2021).
- [44] O. Gamel, *Entangled Bloch spheres: Bloch matrix and two-qubit state space*, Phys. Rev. **A93**, 062320 (2016).
- [45] C. Cafaro and P. M. Alsing, *Information geometry aspects of minimum entropy production paths from quantum mechanical evolutions*, Phys. Rev. **E101**, 022110 (2020).
- [46] C. Cafaro, S. Ray, and P. M. Alsing, *Complexity and efficiency of minimum entropy production probability paths from quantum dynamical evolutions*, Phys. Rev. **E105**, 034143 (2022).
- [47] C. Cafaro and P. M. Alsing, *Complexity of pure and mixed qubit geodesic paths on curved manifolds*, Phys. Rev. **D106**, 096004 (2022).
- [48] A. R. Brown, L. Susskind, and Y. Zhao, *Quantum complexity and negative curvature*, Phys. Rev. **D95**, 045010 (2017).
- [49] S. Chapman, M. P. Heller, H. Marrochio, and F. Pastawski, *Toward a definition of complexity for quantum field theory states*, Phys. Rev. Lett. **120**, 121602 (2018).
- [50] V. Balasubramanian, M. DeCross, A. Kar, and O. Parrikar, *Quantum complexity of time evolution with chaotic Hamiltonians*, J. High Energ. Phys. **2020**, 134 (2020).
- [51] T. Ali, A. Bhattacharyya, S. Shajidul Haque, E. H. Kim, N. Moynihan, and J. Murugan, *Chaos and complexity in quantum mechanics*, Phys. Rev. **D101**, 026021 (2020).
- [52] J. Iaconis, *Quantum state complexity in computationally tractable quantum circuits*, PRX Quantum **2**, 010329 (2021).
- [53] V. Balasubramanian, P. Caputa, J. M. Magan, and Q. Wu, *Quantum chaos and the complexity of spread of states*, Phys. Rev. **D106**, 046007 (2022).
- [54] P. Caputa, J. M. Magan, and D. Patramanis, *Geometry of Krylov complexity*, Phys. Rev. Research **4**, 013041 (2022).

Appendix A: Derivation of $\dot{\mathbf{a}} = 2\mathbf{h} \times \mathbf{a}$

In this Appendix, we present two different derivations of the condition $\dot{\mathbf{a}} = 2\mathbf{h} \times \mathbf{a}$ mentioned in Sections III and IV. The first derivation is based on formal quantum-mechanical rules. The second one, instead, is a rederivation of the original one proposed by Feynman and collaborators in Ref. [1].

1. Abstract derivation

We begin by deriving the relation $\dot{\mathbf{a}} = 2\mathbf{h} \times \mathbf{a}$ with formal quantum-mechanical methods. Consider a nonstationary Hamiltonian defined as $H(t) \stackrel{\text{def}}{=} \mathbf{h}(t) \cdot \boldsymbol{\sigma}$, while the pure state is given by $\rho(t) = |\psi(t)\rangle \langle \psi(t)| = [I + \mathbf{a}(t) \cdot \boldsymbol{\sigma}] / 2$. Recall that the expectation value $\langle Q \rangle_\rho$ of an arbitrary qubit observable $Q \stackrel{\text{def}}{=} q_0 I + \mathbf{q} \cdot \boldsymbol{\sigma}$ with $q_0 \in \mathbb{R}$ and $\mathbf{q} \in \mathbb{R}^3$ is given by $\langle Q \rangle_\rho = q_0 + \mathbf{a} \cdot \mathbf{q}$. Then, the expectation value of the time derivative of the Hamiltonian operator reduces to

$$\langle \dot{H} \rangle = \text{tr} [\rho \dot{H}] = \mathbf{a} \cdot \dot{\mathbf{h}}. \quad (\text{A1})$$

Furthermore, making use of standard quantum mechanics rules, we get

$$\langle \dot{H} \rangle = \partial_t \langle H \rangle = \partial_t (\mathbf{a} \cdot \mathbf{h}) = \dot{\mathbf{a}} \cdot \mathbf{h} + \mathbf{a} \cdot \dot{\mathbf{h}}. \quad (\text{A2})$$

From Eqs. (A1) and (A2), there appears to be a potential incompatibility. Luckily, this is a false suspicion given that $\dot{\mathbf{a}} \cdot \mathbf{h} = 0$ since one can demonstrate that $\dot{\mathbf{a}} = 2\mathbf{h} \times \mathbf{a}$ and, thus, $\dot{\mathbf{a}}$ is orthogonal to \mathbf{h} (and to \mathbf{a}) so that $\dot{\mathbf{a}} \cdot \mathbf{h} = 0$. Therefore, we have to verify that $\dot{\mathbf{a}} = 2\mathbf{h} \times \mathbf{a}$. We start by noting that $\langle \boldsymbol{\sigma} \rangle$ is equal to,

$$\langle \boldsymbol{\sigma} \rangle = \text{tr} [\rho \boldsymbol{\sigma}] = \frac{1}{2} \text{tr} [(\mathbf{a} \cdot \boldsymbol{\sigma}) \boldsymbol{\sigma}] = \mathbf{a}. \quad (\text{A3})$$

Therefore, employing the Schrödinger evolution equation $i\hbar \partial_t |\psi(t)\rangle = H(t) |\psi(t)\rangle$ with $\hbar = 1$, the time derivative of $\langle \boldsymbol{\sigma} \rangle$ in Eq. (A3) becomes

$$\begin{aligned} \dot{\mathbf{a}} &= \partial_t \langle \boldsymbol{\sigma} \rangle \\ &= \partial_t (\langle \psi | \boldsymbol{\sigma} | \psi \rangle) \\ &= \langle \dot{\psi} | \boldsymbol{\sigma} | \psi \rangle + \langle \psi | \boldsymbol{\sigma} | \dot{\psi} \rangle \\ &= i \langle \psi | H \boldsymbol{\sigma} | \psi \rangle - i \langle \psi | \boldsymbol{\sigma} H | \psi \rangle \\ &= i \langle \psi | [H, \boldsymbol{\sigma}] | \psi \rangle, \end{aligned} \quad (\text{A4})$$

that is, the time derivative $\dot{\mathbf{a}}$ of the nonstationary Bloch vector \mathbf{a} reduces to

$$\dot{\mathbf{a}} = i \langle \psi | [H, \boldsymbol{\sigma}] | \psi \rangle. \quad (\text{A5})$$

To further simplify Eq. (A5), we note that the commutator $[H, \sigma_j]$ can be recast as

$$\begin{aligned} [H, \sigma_j] &= [\mathbf{h} \cdot \boldsymbol{\sigma}, \sigma_j] \\ &= [h_i \sigma_i, \sigma_j] \\ &= h_i [\sigma_i, \sigma_j] \\ &= h_i (2i \epsilon_{ijk} \sigma_k) \\ &= -2i \epsilon_{ikj} h_i \sigma_k, \end{aligned} \quad (\text{A6})$$

that is,

$$[H, \sigma_j] = -2i \epsilon_{ikj} h_i \sigma_k, \quad (\text{A7})$$

for any $1 \leq j \leq 3$. Therefore, from Eqs. (A5) and (A7), we obtain

$$\begin{aligned} (\dot{\mathbf{a}})_j &= i (-2i \epsilon_{ikj} h_i \langle \sigma_k \rangle) \\ &= 2 \epsilon_{ikj} h_i a_k \\ &= 2 (\mathbf{h} \times \mathbf{a})_j, \end{aligned} \quad (\text{A8})$$

that is, we arrive at the relation $\dot{\mathbf{a}} = 2\mathbf{h} \times \mathbf{a}$. This equation expresses the fact that the Bloch vector $\mathbf{a}(t)$ rotates about the instantaneous “magnetic field” $\mathbf{h}(t)$ defined by the Hamiltonian $H(t) \stackrel{\text{def}}{=} \mathbf{h}(t) \cdot \boldsymbol{\sigma}$ at each instant of time t . Finally, we end by observing that $\partial_t(\mathbf{a} \cdot \mathbf{h}) = \dot{\mathbf{a}} \cdot \mathbf{h} + \mathbf{a} \cdot \dot{\mathbf{h}} = \mathbf{a} \cdot \dot{\mathbf{h}}$ since $\dot{\mathbf{a}} \cdot \mathbf{h} = 0$ because $\dot{\mathbf{a}} = 2\mathbf{h} \times \mathbf{a}$ is perpendicular to the vector \mathbf{h} .

In what follows, we present an alternative derivation of the condition $\dot{\mathbf{a}} = 2\mathbf{h} \times \mathbf{a}$ inspired by the original calculation by Feynman and collaborators in Ref. [1].

2. Feynman’s derivation

In Ref. [1], Feynman and collaborators showed how the dynamics of a two-level quantum system in a time-dependent background can be geometrically described in terms of two real three-dimensional vectors, the unit Bloch vector $\mathbf{r}(t)$ and a vector $\boldsymbol{\Omega}(t)$ that specifies the perturbation. More specifically, consider a two-level quantum system whose evolution is governed by the Schrödinger equation given by,

$$i\hbar\partial_t|\psi\rangle = (\mathbf{H}_0 + V)|\psi\rangle, \quad (\text{A9})$$

with $\mathbf{H}_0 \stackrel{\text{def}}{=} (\hbar\omega_0/2)\sigma_z$ and $V = V(t)$ being a time-dependent perturbation. Observe that the full Hamiltonian $H(t) \stackrel{\text{def}}{=} \mathbf{H}_0 + V(t)$ can also be recast as $H(t) \stackrel{\text{def}}{=} (\hbar/2)\boldsymbol{\Omega}(t) \cdot \boldsymbol{\sigma}$. Assume that $|\psi\rangle \stackrel{\text{def}}{=} a(t)|\psi_a\rangle + b(t)|\psi_b\rangle$ with $\{|\psi_a\rangle, |\psi_b\rangle\}$ being an orthonormal basis for the Hilbert space of single-qubit quantum states, where $a(t)$ and $b(t)$ are complex probability amplitudes satisfying the normalization condition $|a(t)|^2 + |b(t)|^2 = 1$. In matrix representation, the Schrödinger equation in Eq. (A9) becomes,

$$\begin{pmatrix} i\hbar\frac{da}{dt} \\ i\hbar\frac{db}{dt} \end{pmatrix} = \begin{pmatrix} \frac{\hbar\omega_0}{2} + V_{aa} & V_{ab} \\ V_{ba} & -\frac{\hbar\omega_0}{2} + V_{bb} \end{pmatrix} \begin{pmatrix} a(t) \\ b(t) \end{pmatrix}, \quad (\text{A10})$$

where $V_{ij}(t) \stackrel{\text{def}}{=} \langle\psi_i|V(t)|\psi_j\rangle$, $\langle\psi_i|\psi_j\rangle = \delta_{ij}$, and $i, j \in \{a, b\}$. Therefore, the four scalar equations emerging from Eq. (A10) are

$$\begin{aligned} i\hbar\frac{da}{dt} &= \left(\frac{\hbar\omega_0}{2} + V_{aa}\right)a(t) + V_{ab}b(t), \\ i\hbar\frac{db}{dt} &= V_{ba}a(t) + \left(-\frac{\hbar\omega_0}{2} + V_{bb}\right)b(t), \\ -i\hbar\frac{da^*}{dt} &= \left(\frac{\hbar\omega_0}{2} + V_{aa}\right)a^*(t) + V_{ba}b^*(t), \\ -i\hbar\frac{db^*}{dt} &= V_{ab}a^*(t) + \left(-\frac{\hbar\omega_0}{2} + V_{bb}\right)b^*(t). \end{aligned} \quad (\text{A11})$$

For later use, we also remark that from $(\hbar/2)\boldsymbol{\Omega}(t) \cdot \boldsymbol{\sigma} = \mathbf{H}_0 + V(t)$ and Eq. (A10), we have

$$\boldsymbol{\Omega} \stackrel{\text{def}}{=} \left(\frac{V_{ab} + V_{ba}}{\hbar}, i\frac{V_{ab} - V_{ba}}{\hbar}, \omega_0 + \frac{V_{aa} - V_{bb}}{\hbar}\right). \quad (\text{A12})$$

In the majority of cases of interest, $V_{aa} = V_{bb} = 0$ or, alternatively, V_{aa} and V_{bb} are negligible compared to $(\hbar/2)\omega_0$. Remarkably, putting $\rho(t) = |\psi(t)\rangle\langle\psi(t)| = [I + \mathbf{r}(t) \cdot \boldsymbol{\sigma}]/2$, Feynman and collaborators were the first to point out that Eq. (A9) can be geometrically recast as

$$\dot{\mathbf{r}} = \boldsymbol{\Omega} \times \mathbf{r}, \quad (\text{A13})$$

that is, as

$$\frac{dx}{dt} = \Omega_y z - \Omega_z y, \quad \frac{dy}{dt} = \Omega_z x - \Omega_x z, \quad \frac{dz}{dt} = \Omega_x y - \Omega_y x, \quad (\text{A14})$$

where $\mathbf{r} = (x, y, z)$ is the unit Bloch vector. The real three-dimensional vector \mathbf{r} is defined as

$$\mathbf{r} \stackrel{\text{def}}{=} (ab^* + ba^*, i(ab^* - ba^*), |a|^2 - |b|^2), \quad (\text{A15})$$

while $\boldsymbol{\Omega}$ is given in Eq. (A12). From Eq. (A15), one can explicitly verify that $\mathbf{r} \cdot \mathbf{r} = 1$ thanks to the fact that $|a(t)|^2 + |b(t)|^2 = 1$. Moreover, given the Hermiticity of the perturbation operator $V(t)$, one also has that $V_{aa} = V_{aa}^*$, $V_{ab} = V_{ba}^*$, $V_{ba} = V_{ab}^*$, and $V_{bb} = V_{bb}^*$. For completeness, we check here the first relation in Eq. (A14). Specifically, we wish to verify that $dx/dt = \Omega_y z - \Omega_z y$, that is

$$\frac{d(ab^* + ba^*)}{dt} = i \frac{V_{ab} - V_{ba}}{\hbar} (|a|^2 - |b|^2) - i \left(\omega_0 + \frac{V_{aa} - V_{bb}}{\hbar} \right) (ab^* - ba^*). \quad (\text{A16})$$

Note that Eq. (A16) is correct if and only if,

$$\begin{aligned} -i\hbar \frac{d(ab^* + ba^*)}{dt} &= -i\hbar \left(\frac{da}{dt} b^* + a \frac{db^*}{dt} + \frac{db}{dt} a^* + b \frac{da^*}{dt} \right) \\ &= (V_{ab} - V_{ba}) (|a|^2 - |b|^2) - (\hbar\omega_0 + V_{aa} - V_{bb}) (ab^* - ba^*). \end{aligned} \quad (\text{A17})$$

At this point, note that

$$\begin{aligned} -i\hbar \frac{d(ab^* + ba^*)}{dt} &= -i\hbar b^* \left(\frac{da}{dt} \right) - i\hbar a \left(\frac{db^*}{dt} \right) - i\hbar a^* \left(\frac{db}{dt} \right) - i\hbar b \left(\frac{da^*}{dt} \right) \\ &= -b^* \left(i\hbar \frac{da}{dt} \right) + a \left(-i\hbar \frac{db^*}{dt} \right) - a^* \left(i\hbar \frac{db}{dt} \right) + b \left(-i\hbar \frac{da^*}{dt} \right) \\ &= -b^* \left[\left(\frac{\hbar\omega_0}{2} + V_{aa} \right) a + V_{ab} b \right] + a \left[V_{ab} a^* + \left(-\frac{\hbar\omega_0}{2} + V_{bb} \right) b^* \right] + \\ &\quad - a^* \left[V_{ba} a + \left(-\frac{\hbar\omega_0}{2} + V_{bb} \right) b \right] + b \left[\left(\frac{\hbar\omega_0}{2} + V_{aa} \right) a^* + V_{ba} b^* \right] \\ &= -ab^* \frac{\hbar\omega_0}{2} - ab^* V_{aa} - |b|^2 V_{ab} + |a|^2 V_{ab} - \frac{\hbar\omega_0}{2} ab^* + ab^* V_{bb} + \\ &\quad - |a|^2 V_{ba} + a^* b \frac{\hbar\omega_0}{2} - a^* b V_{bb} + a^* b \frac{\hbar\omega_0}{2} + a^* b V_{aa} + V_{ba} |b|^2 \\ &= (V_{ab} - V_{ba}) (|a|^2 - |b|^2) - \hbar\omega_0 (ab^* - ba^*) + (V_{aa} - V_{bb}) (a^* b - ab^*), \end{aligned} \quad (\text{A18})$$

that is,

$$-i\hbar \frac{d(ab^* + ba^*)}{dt} = (V_{ab} - V_{ba}) (|a|^2 - |b|^2) - \hbar\omega_0 (ab^* - ba^*) + (V_{aa} - V_{bb}) (a^* b - ab^*). \quad (\text{A19})$$

Therefore, using Eqs. (A17) and (A19), it happens that the relation $dx/dt = \Omega_y z - \Omega_z y$ holds true. The remaining two relations in Eq. (A14) can be verified in a similar fashion. As a final remark, we note that $\dot{\mathbf{r}} = \boldsymbol{\Omega} \times \mathbf{r}$ for the Hamiltonian $H(t) \stackrel{\text{def}}{=} (\hbar/2)\boldsymbol{\Omega}(t) \cdot \boldsymbol{\sigma}$ reduces to the condition $\dot{\mathbf{a}} = 2\mathbf{h} \times \mathbf{a}$ for the Hamiltonian $H(t) \stackrel{\text{def}}{=} \mathbf{h}(t) \cdot \boldsymbol{\sigma}$ once we consider the correspondences $\mathbf{r} \leftrightarrow \mathbf{a}$, $\boldsymbol{\Omega}/2 \leftrightarrow \mathbf{h}$, and set $\hbar = 1$. With this last remark, we end our two derivations.